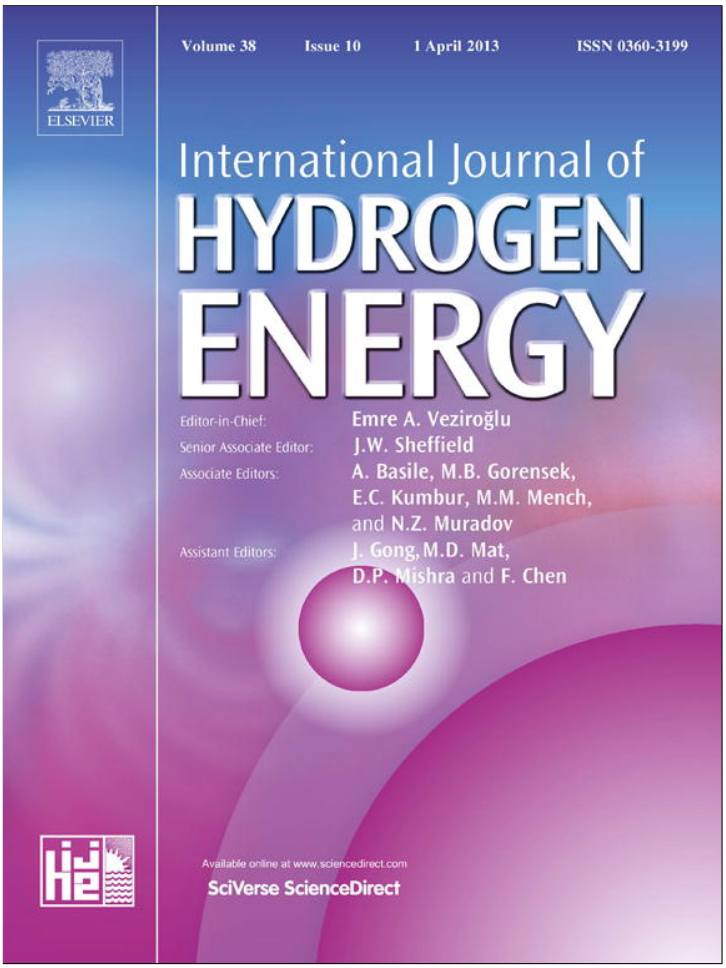

INTERNATIONAL JOURNAL OF HYDROGEN ENERGY 38 (2013) 4177–4184

Available online at www.sciencedirect.com

SciVerse ScienceDirect

journal homepage: www.elsevier.com/locate/he

Self-ignition of hydrocarbon–hydrogen–air mixtures

S.M. Frolov *, S.N. Medvedev, V.Ya. Basevich, F.S. Frolov

Semenov Institute of Chemical Physics, Russian Academy of Sciences, 4 Kosygin Str., Moscow 119991, Russia

ARTICLE INFO

Article history:
Received 30 October 2012
Received in revised form
6 January 2013
Accepted 11 January 2013
Available online 16 February 2013

Keywords:
Triple hydrogen–hydrocarbon–air mixture
Heavy hydrocarbon
Self-ignition
Detailed kinetic mechanism
Numerical simulation

ABSTRACT

The effect of hydrogen admixing on self-ignition of homogeneous and hybrid mixtures of heavy hydrocarbons in air is studied theoretically based on the detailed reaction mechanism of *n*-decane oxidation. Reactivity of hydrogen-containing mixtures is not always higher than that of pure hydrocarbon–air mixtures. At temperatures less than ~1050 K, addition of hydrogen to such mixtures increases the self-ignition delay: hydrogen acts as an inhibitor. With the increase of hydrogen content the duration of the blue-flame reaction stage becomes shorter and even degenerates. This is caused by reactions of hydrogen with intermediate products of hydrocarbon oxidation leading to formation of less active species hindering chain branching processes. At temperatures exceeding ~1050 K, hydrogen addition decreases the overall self-ignition delay thus indicating that hydrogen acts as a promoter. These finding have to be taken into account when discussing perspectives of practical applications of fuels blended with hydrogen as well as related explosion safety issues.

1. Introduction

Hydrogen exhibits unique properties – low density (0.08 kg/m^3 at 300 K and 1 atm), wide flammability limits (from 4% (vol.) to 75% (vol.) in air), high laminar flame velocity (2.3 m/s at normal conditions) and very low ignition energy (0.02 mJ). In addition, combustion of hydrogen–air mixtures is known to be accompanied with formation of only nitrogen oxides as pollutants and at fuel–air ratio $\Phi < 0.5$ their emissions nearly vanish. Therefore the idea of partial or complete replacement of hydrocarbon fuel with hydrogen in power plants and transportation engines is currently actively discussed in the literature [1]. However the relevant literature contains contradictory information on the effects of hydrogen on hydrocarbon fuel ignition and combustion.

For example, diesel engine performances under the operation on diesel oil blended with different secondary gaseous fuels were reported in [2]. Propane, methane, ethanol, and hydrogen were chosen as the secondary fuels. Self-ignition and combustion characteristics of blended fuels as well as emissions of NO_x, CO and unreacted hydrocarbons were measured experimentally. The conclusion was made that using the knowledge of combustion characteristics of blended fuels to properly tune the operation process one can reduce considerably pollutant emissions and decrease the self-ignition delay.

In [3], experiments and numerical simulation of piston engine operation on *n*-heptane blended with hydrogen were performed to find out whether hydrogen addition decreases NO_x emissions. As a matter of fact, hydrogen addition was shown to reduce NO emission but NO_2 emission appeared to be higher than that for the unblended fuel. Moreover, the ultimate emission of NO_x also increased. Numerical simulations were unable to adequately predict the NO_x emission level. To explain these findings, the author of [3] assumed that the increase of NO_2 concentration in the course of combustion of blended fuel is caused by higher concentrations of HO_2 radical serving as an oxidizing agent for NO. Note that hydrogen

* *Corresponding author*. Tel.: +7 495 9397228.
E-mail addresses: smfrol@chph.ras.ru, sergei@frolovs.ru (S.M. Frolov).
0360-3199/$ – see front matter
http://dx.doi.org/10.1016/j.ijhydene.2013.01.075

Nomenclature

A	preexponential factor in Arrhenius expression for reaction rate, mol, m^3, s
c	specific heat, J/kg/K
D	diffusion coefficient, m^2/s
E	activation energy in Arrhenius expression for reaction rate, J/mol
H	heat effect of chemical reaction, J/kg
L	number of chemical reactions
L_v	latent heat of vaporization, J/kg
m	mass of fuel drop, kg
N	number of chemical species
n	power exponent in Arrhenius expression for reaction rate
r	radial coordinate, m
u	velocity, m/s
P	pressure, Pa
R	effective half-distance between drops, m
R^o	universal gas constant, J/mol/K
T	temperature, K
t	time, s
t_{ign}	ignition delay, s
$t_{ign,\ calc}$	predicted ignition delay, s
$t_{ign,\ exp}$	measured ignition delay, s
W	molecular mass, kg/kmol
Y	species mass fraction
λ	thermal conductivity, W/m/K
Φ	fuel–air ratio
φ_{st}	stoichiometric fuel–air ratio
ρ	density, kg/m^3
η	mass content of liquid in the unit volume of drop suspension, kg/m^3
Ω	chemical heat source, W/m^3
ω	rate of variation of species mass fractions due to chemical reactions, $kg/m^3/s$

Indices

0	initial value
d	relates to liquid
g	relates to gas
j	relates to species
k	relates to reaction
s	relates to drop surface
v	relates to liquid vapor

addition resulted in the reduction of emissions of soot, CO, CO_2, and unreacted hydrocarbons.

Despite self-ignition and combustion characteristics of hydrogen and many individual hydrocarbons are fairly well studied, there is not much data for hydrocarbon–hydrogen blends related to their explosion safety. As a matter of fact, only limited data are available on blended fuel combustion (e.g., methane–hydrogen [4], propane–hydrogen [5], kerosene–hydrogen [6,7]) and self-ignition (methane–hydrogen [8]). Surprisingly, the fact that hydrogen reactivity in air is not always higher than that of hydrocarbons, in particular at low temperatures, is not discussed at all in the relevant literature.

The objective of this paper is the theoretical study of the effect of hydrogen admixing on self-ignition of homogeneous and hybrid mixtures of heavy hydrocarbons (*n*-heptane and *n*-decane) in air based on the well-validated detailed reaction mechanism of *n*-decane oxidation.

2. Chemical reaction mechanism

For modeling the effect of hydrogen additives to homogeneous and hybrid (with liquid drops) mixtures of heavy hydrocarbons (*n*-heptane and *n*-decane) with air on self-ignition we used a well-validated, relatively compact detailed reaction mechanism of *n*-decane oxidation developed at Semenov Institute of Chemical Physics [9]. This mechanism contains only 1083 elementary processes that govern the reaction rate and the formation of basic intermediate and final products represented by 108 species. The mechanism has two essential features: (i) reactions of so called double addition of oxygen (first, to the alkyl radical, then to the isomerized form of the formed alkylperoxide radical) are lacking because the first addition is considered to be sufficient; (ii) isomeric compounds and their derivative substances as intermediate species are not considered, because this means of oxidation is slower than through molecules and radicals of the normal structure. This mechanism was systematically validated for propane [10], *n*-butane [11], *n*-pentane [12], *n*-hexane [13], *n*-heptane [14], and *n*-decane [9]. The major feature of this mechanism is the appearance of stages, viz., cool and blue flames during low-temperature self-ignition.

To show the performance of the mechanism we present here some examples with the self-ignition of homogeneous mixtures using the kinetic code KINET developed at Semenov Institute of Chemical Physics [15]. The code solves zero-dimensional time dependent equations of chemical kinetics coupled with the energy conservation equation for isobaric conditions.

Fig. 1a presents typical calculated time dependences of temperature during the spontaneous ignition of a stoichiometric *n*-decane–air mixture, which are characteristic for low and high initial temperatures. The first stepped increase for the relatively low initial temperature $T_0 = 588$ K at $t \sim 1.27$ s is related to the appearance of the cool flame. The blue flame (clearly visible in Fig. 1b with a change of the scale) then appears after a lapse of about 0.28 s; the hot flame then appears at approximately 1.57 s and the temperature increases to 2500 K and higher. The stages of spontaneous ignition, i.e. stepwise appearance of cool, blue, and hot flames, occur as follows. The acceleration of the reaction in the cool flame is the consequence of branching during decomposition of alkyl hydroperoxide (here, alkyl hydroperoxide $C_{10}H_{21}O_2H$) with the formation of hydroxyl and oxyradical. The appearance of the blue flame is the consequence of branching because of the decomposition of hydrogen peroxide H_2O_2. This is clearly evident in Fig. 1b from the calculated kinetic curves for peroxide and the two peaks in the concentration of hydroxyl. The stages result in the phenomenon of the negative temperature coefficient (NTC) of the reaction rate; the overall self-ignition

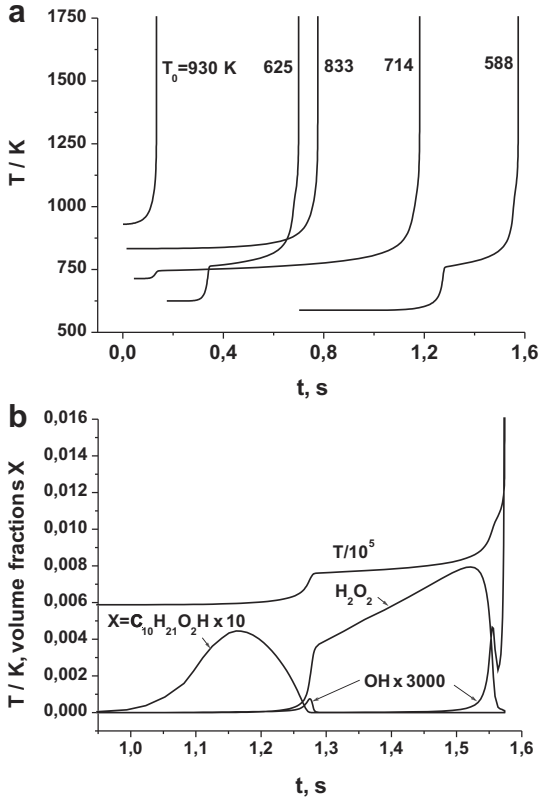

Fig. 1 – Calculations of spontaneous ignition of stoichiometric *n*-decane–air mixture at initial pressure $P_0 = 1$ atm: (a) time histories of temperature at $T_0 = 588$, 625, 714, 833, and 930 K; and (b) time histories of temperature and volume fractions of peroxides and hydroxyl at $T_0 = 588$ K.

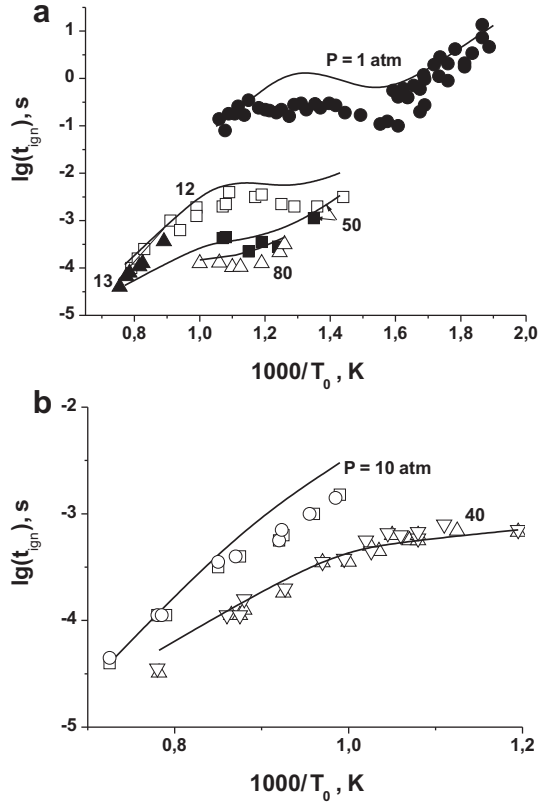

Fig. 2 – Comparison of measured (points) and calculated (curves) overall self-ignition delays of stoichiometric *n*-decane–air mixture at different temperatures and pressures: (a) experiments [16–18]; and (b) experiments [19,20].

delays at a higher initial temperature appear to be greater than at a low temperature. This effect is clearly seen in Fig. 1a. Note that in the calculations, the overall self-ignition delay time t_{ign} was determined as the time taken for the temperature growth rate to attain the value of 10^7 K/s. Other possible definitions (10^6 K/s and max(dT/dt)) were proved to give very similar results for t_{ign}.

Fig. 2a and b compare calculated (curves) and measured (points) overall self-ignition delays t_{ign} for various initial temperatures and pressures. In all cases, the homogeneous mixture composition is stoichiometric (1.33% $C_{10}H_{22}$–air). The points on the graphs correspond to the experimental data of [16] for pressures of 12 and 50 atm, experimental data of [17] for pressures of 13 and 80 atm, experimental data of [18] for a pressure of 1 atm (see Fig. 2a), and experimental data of [19,20] for pressures of 10 and 40 atm (Fig. 2b).

It follows from Fig. 2 that the detailed reaction mechanism of *n*-decane oxidation provides satisfactory agreement with available experimental data on overall self-ignition delays in wide ranges of initial temperature and pressure. Note that hydrogen oxidation kinetics is included in the *n*-decane oxidation mechanism as a constituent part. Fig. 3a demonstrates the performance of the hydrogen oxidation kinetics by means of comparison between calculated (curve) and measured (points) self-ignition delays for stoichiometric hydrogen–air mixture at different initial temperatures and pressure $P_0 = 1$ atm. In addition, Fig. 3b compares predicted $t_{ign,\ calc}$ and measured $t_{ign,\ exp}$ ignition delays of different hydrogen–oxygen–diluent mixtures in wide ranges of pressure (up to 50 atm) and temperature at the plane $t_{ign,\ calc}$ vs. $t_{ign,\ exp}$. The straight line corresponds to the condition $t_{ign,\ calc} = t_{ign,\ exp}$, whereas each point in Fig. 3b represents the actual relationship between $t_{ign,\ calc}$ and $t_{ign,\ exp}$ for the same thermochemical conditions as in the corresponding experiments [23–29]. Clearly, the line $t_{ign,\ calc} = t_{ign,\ exp}$ is within the scatter of points in Fig. 3b but tends to be closer to the lower margin of the scatter, in particular at low temperatures.

3. Model of drop self-ignition and combustion [30]

The liquid drop is assumed to be a sphere of radius r_s and occupy the region $0 < r < r_s$ at time t (index s relates to drop surface). The droplet size is allowed to vary in time due to thermal expansion and liquid vaporization processes. Therefore, r_s is treated as the moving boundary.

The continuity equation for liquid is

$$\frac{\partial \rho_d}{\partial t} + \frac{1}{r^2}\frac{\partial}{\partial r}\left(r^2 \rho_d u_d\right) = 0 \qquad (1)$$

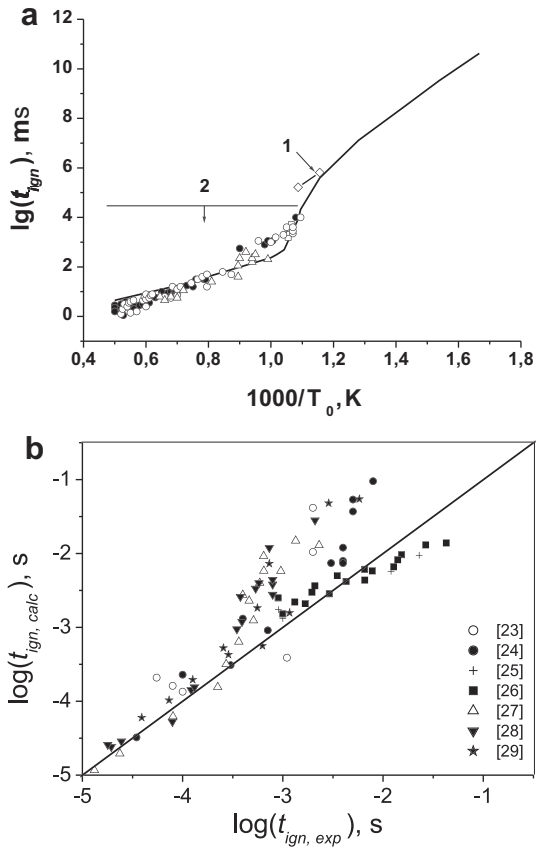

Fig. 3 – (a) Comparison of measured (points) and calculated (curve) self-ignition delays of stoichiometric hydrogen–air mixture at different temperatures and $P_0 = 1$ atm: 1 – experiments cited in [21]; and 2 – experiments [22]; (b) comparison of predicted t_{ign}(calc.) and measured t_{ign}(exp.) ignition delays of different hydrogen–oxygen–diluent mixtures in wide ranges of pressure and temperature. Experimental values are taken from [23–29].

where index d relates to liquid, r is the radial coordinate, ρ is the density, and u is the velocity.

Temperature distribution in liquid ($0 < r < r_s$), $T_d(r)$ is governed by the energy equation:

$$c_d\rho_d\frac{\partial T_d}{\partial t} + c_d\rho_d u_d\frac{\partial T_d}{\partial r} = \frac{1}{r^2}\frac{\partial}{\partial r}\left(\lambda_d r^2\frac{\partial T_d}{\partial r}\right), \tag{2}$$

$$T_d(0,r) = T_{d0}, \quad \left.\frac{\partial T_d}{\partial r}\right|_{r=0} = 0, \quad T_d(t,r_s) = T_g(t,r_s),$$

where T is the temperature, c is the specific heat, and λ is the thermal conductivity.

The mass fraction of liquid vapor (index v) at the drop surface is

$$Y_v = \frac{P_v}{P}\frac{W_v}{\overline{W}}, \tag{3}$$

where P is the pressure, P_v is the saturated vapor pressure, W is the molecular mass, and bar denotes the mean value.

The gas phase (index g) is assumed to occupy region $r_s < r < R$, where R is the effective half-distance between drops in gas–drop suspension. This parameter can be found based on the simple formula [30]

$$R = r_{s0}\left(\frac{\rho_d}{\eta}\right)^{1/3} = r_{s0}\left(\frac{\rho_d}{\rho_g\Phi\varphi_{st}}\right)^{1/3} \tag{4}$$

where index 0 denotes the initial value, η is the mass content of liquid in the unit volume of drop suspension, Φ is the fuel–air ratio, and φ_{st} is the stoichiometric fuel–air ratio ($\varphi_{st} \approx 0.06$ for hydrocarbon fuels).

The gas flow around the drop is governed by the continuity equation

$$\frac{\partial\rho_g}{\partial t} + \frac{1}{r^2}\frac{\partial}{\partial r}\left(r^2\rho_g u_g\right) = 0, \tag{5}$$

$$\rho_d\left(u_d - \frac{\partial r_s}{\partial t}\right)\Big|_{r=r_s} = \rho_g\left(u_g - \frac{\partial r_s}{\partial t}\right)\Big|_{r=r_s},$$

species continuity equation

$$\rho_g\frac{\partial Y_j}{\partial t} = \frac{1}{r^2}\frac{\partial}{\partial r}\left(\rho_g r^2 Y_j V_j\right) - \rho_g u_g\frac{\partial Y_g}{\partial r} + \omega_{gj} \tag{6}$$

$$Y_j(0,r) = Y_{j0} \quad j = 1,2,\ldots,N,$$

$$-\rho_d u_i\beta_j\big|_{r=r_s} = \rho_g Y_j\left(u_g - \frac{\partial r_s}{\partial t}\right) + \rho_g Y_j V_j\Big|_{r=r_s}, \tag{7}$$

$$\left.\frac{\partial\overline{W}Y_j}{\partial r}\right|_{r=R} = 0, \quad j = 1,\ldots,N$$

$$X_j = Y_j\overline{W}/W_j \tag{8}$$

$$\frac{\partial X_j}{\partial r} = \sum_{k=1}^{N}\left(\frac{X_j X_k}{D_{jk}}\right)(V_k - V_j) \tag{9}$$

$$\omega_{gj} = W_{gj}\sum_{k=1}^{L}\left(\nu''_{j,k} - \nu'_{j,k}\right)A_k T_g^{n_k}\exp\left(-\frac{E_k}{R^o T_g}\right)\prod_{l=1}^{N}\left(\frac{Y_{gl}\rho_g}{W_{gl}}\right)^{\nu'_{l,k}} \tag{10}$$

$$\beta_j = 1 \text{ at } j = v$$

$$\beta_j = 0 \text{ at } j \neq v$$

and energy equation

$$c_{pg}\rho_g\frac{\partial T_g}{\partial t} = \frac{1}{r^2}\frac{\partial}{\partial r}\left(\lambda_g r^2\frac{\partial T_g}{\partial r}\right) - c_{pg}\rho_g u_g\frac{\partial T_g}{\partial r} + \Omega \tag{11}$$

$$T_g(0,r) = T_{g0}$$

$$T_g(t,r_s) = T_d(t,r_s), \quad \left.\frac{\partial T_g}{\partial r}\right|_{r=R} = 0$$

$$\Omega = \sum_{k=1}^{L} H_k A_k T_g^{n_k}\exp\left(-\frac{E_k}{R^o T_g}\right)\prod_{j=1}^{N}\left(\frac{Y_{gj}\rho_g}{G_{gj}}\right)^{\nu'_{j,k}},$$

where Y_j is the mass fraction of species j; D_j is the diffusion coefficient for species j; ω_j is the rate of variation of mass fraction of species j due to chemical reactions; Ω is the chemical heat source; A_k, n_k, E_k, and H_k are the preexponential

factor, power exponent, activation energy, and heat effect of the kth reaction; N is the number of species; L is the number of reactions, respectively.

In addition to above equations, the boundary condition for tailoring temperature fields in liquid and gas at $r = r_s$

$$\lambda_d \frac{\partial T_d}{\partial r} - \frac{\rho_{ds} u_s L_v}{W_v} = \lambda_g \frac{\partial T_g}{\partial r}, \tag{12}$$

equation of state for the gas phase

$$\rho_g = \frac{P\overline{W}}{R^o T_g}, \tag{13}$$

and the condition of constant pressure

$$P = P_0 = \text{const} \tag{14}$$

are specified. Here, L_v is the latent heat of vaporization and R^o is the universal gas constant.

Molecular transport processes in liquid and gas phases as well as the corresponding specific heats are taken from [31].

To study ignition and combustion of hydrocarbon fuel drops in air, the detailed reaction mechanism of n-decane oxidation discussed in Section 2 was used.

The set of governing equations was integrated numerically using DROP code developed at Semenov Institute of Chemical Physics. Applied in the code is a nonconservative finite-difference scheme and adaptive moving grid. The computational error was continuously monitored by checking balances of C and H atoms as well as energy balance at each time step. More details on the computational procedure can be found in [30].

The model described above was validated against experimental data on drop self-ignition and combustion for various liquid hydrocarbons. As an example, Fig. 4 compares the calculated (curve) and measured (points [32,33]) dependences of the overall ignition delay time t_{ign} for n-heptane drops. The definition of t_{ign} was the same as for the homogeneous mixtures but the criterion 10^7 K/s for the temperature growth rate was applied to the maximum gas temperature $T_{g,max}(t)$. As can be seen, the overall self-ignition delay time increases sharply at low pressures. Furthermore, Fig. 5 compares the calculated (curves) and measured (points from [34]) delay times of cool flame appearance (t_{cf}) and overall self-ignition delay time (t_{ign}) for n-decane drops of initial diameter 700 μm at different initial temperatures and pressure $P_0 = 1$ atm. The delay time of cool flame appearance (t_{cf}) was defined as the time taken for the maximum gas temperature $T_{g,max}$ to attain the inflection point at the first stepwise temperature variation in the $T_{g,max} - t$ plane. Clearly, the model predicts correctly not only qualitative features of drop self-ignition phenomenon but also provides satisfactory quantitative information. Note that cool flames during self-ignition of liquid sprays were observed experimentally long ago [35].

4. Self-ignition of homogeneous hydrocarbon–hydrogen–air mixtures

The reaction mechanism of Section 2 was first used to study the effect of hydrogen addition on the self-ignition delay time of homogeneous hydrocarbon–air mixtures. The calculations of mixture self-ignition and volumetric combustion were performed using KINET code.

Fig. 6 shows the predicted dependences of overall self-ignition delays on temperature for homogeneous stoichiometric n-heptane–air mixtures with different content of hydrogen (from 0% (vol.) to 100% (vol.)) at pressure $P_0 = 15$ atm. At $T_0 \approx 1050$ K, the self-ignition delays of n-heptane–air and hydrogen–air mixtures are seen to be the same. At $T_0 < 1050$ K, addition of hydrogen to n-heptane–air mixture increases the self-ignition delay, whereas at $T_0 > 1050$ K, decreases it. Note that even in the mixtures with high amount of hydrogen (e. g., 95% (vol.)), the effect of NTC of reaction rate is clearly seen in Fig. 6. It is worth to remind here that according to Fig. 3b the hydrogen oxidation kinetics embedded in the hydrocarbon oxidation mechanism tends to predict the ignition delays of hydrogen somewhat larger than the average

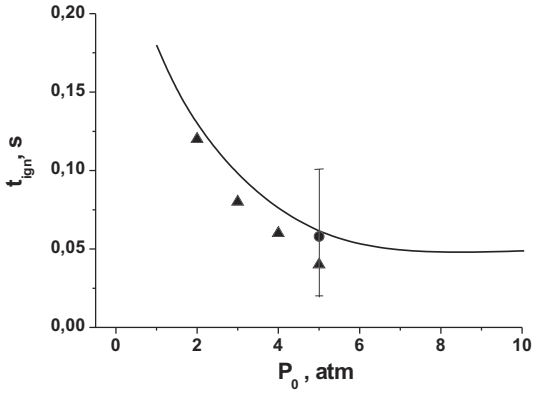

Fig. 4 – Calculated pressure dependence (curve) of self-ignition delay time t_{ign} for n-heptane drops with $d_0 = 700$ μm at $T_0 = 1000$ K against experimental data. Triangles – measured values of t_{ign} for single n-heptane drops with $d_0 = 700$–750 μm and $T_0 = 1000$ K [32]; circle – for drops with $d_0 = 700$ μm and $T_0 = 940$ K [33] (the vertical bar indicates the scatter in experimental data).

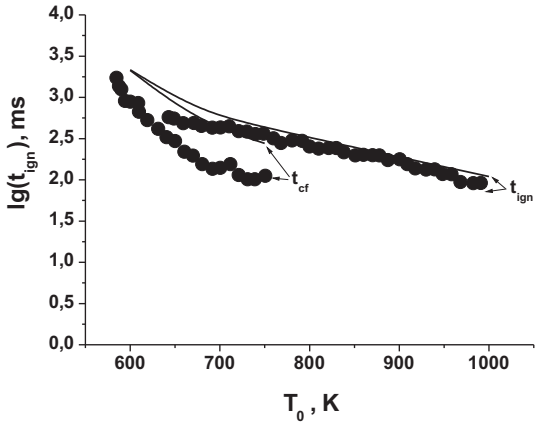

Fig. 5 – Comparison of calculated (curves) and measured (points [34]) dependences of the delay times of cool flame (t_{cf}) and hot flame (t_{ign}) appearance on the initial temperature for a single n-decane drop in air: $d_0 = 700$ μm and $P_0 = 1$ atm.

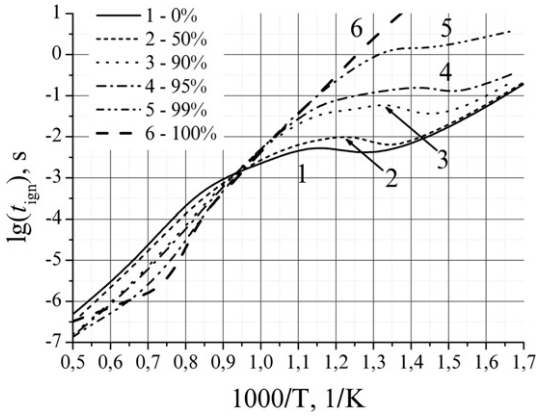

Fig. 6 – Predicted dependences of self-ignition delays on temperature for stoichiometric homogeneous C_7H_{16}–H_2–air mixtures with different hydrogen content: 1 – 0% (vol.), 2 – 50%, 3 – 90%, 4 – 95%, 5 – 99%, and 6 – 100%; pressure P_0 = 15 atm.

measured values, in particular at low temperatures. This means that in reality the ignition inhibiting effect of hydrogen at $T_0 < 1050$ K could be even more pronounced than derived here.

5. Self-ignition of hybrid hydrocarbon (drops) – hydrogen – air mixtures

The reaction mechanism of Section 2 was then used to study the effect of hydrogen addition on the self-ignition delay time of hybrid hydrocarbon drops–hydrogen–air mixtures. The calculations of ignition and combustion of such mixtures were performed using DROP code.

Fig. 7 shows the predicted time histories of the maximum gas temperature $T_{g,max}$ at self-ignition of hybrid stoichiometric compositions containing *n*-heptane drops, air, and hydrogen with different volumetric content: 0%, 7.5%, and 14.75%. The calculations were made for drops of $d_0 = 60$ μm at $T_0 = 1000$ K, and $P_0 = 20$ atm.

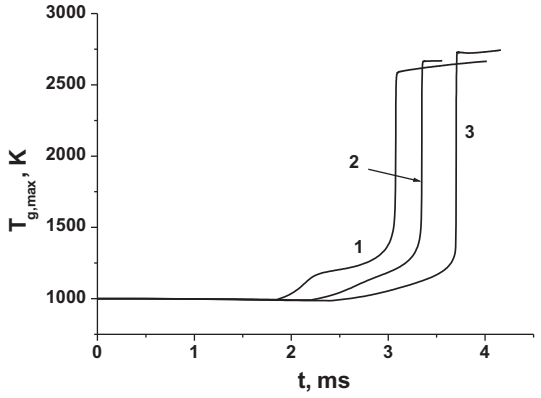

Fig. 7 – Predicted time histories of the maximum gas temperature $T_{g,max}$ in the stoichiometric mixture *n*-heptane (drops) – hydrogen – air at different initial hydrogen content: 1 – 0% (vol.), 2 – 7.5% (vol.), and 3 – 14.75% (vol.); d_0 = 60 μm, P_0 = 20 atm, and T_{g0} = 1000 K.

The stoichiometric composition of hybrid mixture was set according to the following procedure. First, the volume of air needed for complete oxidation of hydrocarbon fuel was determined. Then, a certain amount of hydrogen was added to this volume of air. Finally, the resultant homogeneous hydrogen–air mixture was diluted with such an amount of additional air which was needed for complete oxidation of hydrogen. Based on this procedure, the volume fraction of hydrogen in the gas phase was determined.

The analysis of spatial distributions of intermediate reaction products indicates that the staged behavior of the maximum gas temperature $T_{g,max}$ in Fig. 7 is caused by the appearance of the blue flame due to decomposition of hydrogen peroxide accumulated in a local region in the close vicinity to the drop surface. With the increase of hydrogen content in the hybrid mixture, the duration of the blue-flame reaction stage becomes shorter and the overall self-ignition delay time increases. When taking Fig. 6 into account, this result could be treated as trivial because at $T_0 = 1000$ K the overall self-ignition delay in the homogeneous stoichiometric *n*-heptane – air mixture is approximately a factor of 2 shorter than that in the homogeneous stoichiometric hydrogen – air mixture. However one has to keep in mind that Fig. 7 relates to the self-ignition of hybrid rather than homogeneous mixture. At self-ignition of liquid drops the temperature and fuel vapor concentration in the vicinity of the drop surface are highly nonuniform. Moreover, self-ignition of fuel vapor occurs in the region where the gas temperature is lower than its value at a large distance from the drop surface and the fuel vapor – air mixture is essentially fuel lean [30]. In view of it, the results of Fig. 7 are not trivial. Note also that the degeneration of the blue flame stage of *n*-heptane oxidation is caused by reactions of molecular hydrogen with the intermediate products of fuel oxidation, in particular with alkyl hydroperoxides, hydrogen peroxide and products of their decomposition leading to the formation of less active radicals like HO_2.

These considerations are confirmed by the results of calculations presented in Fig. 8. Shown in Fig. 8 are the predicted time histories of maximum gas temperature at self-ignition of *n*-heptane (Fig. 8a) and *n*-decane (Fig. 8b) drop suspensions in air mixed with 7.5% (vol.) hydrogen (solid curves) and in pure air (dashed curves) at $P_0 = 20$ atm and different initial temperatures. It is clearly seen that hydrogen addition affects not only the overall self-ignition delay time t_{ign} but also the duration of intermediate stages of multistage self-ignition (cool and blue flames). At a relatively low temperature (e. g., at $T_0 = 800$ K) the duration of cool and blue flame stages increases considerably. This indicates that molecular hydrogen deactivates active intermediate radicals participating in the channels of chain origination, propagation, and branching. Nevertheless, similar to homogeneous mixtures, at $T_0 < 1050$ K, the self-ignition delay time in the hydrogen-containing hybrid mixtures increases as compared to the mixtures without hydrogen, whereas at $T_0 > 1050$ K, it decreases.

The detailed analysis of various physical and chemical processes in the vicinity to the drop surface reveals several more interesting features of hybrid mixture self-ignition. For

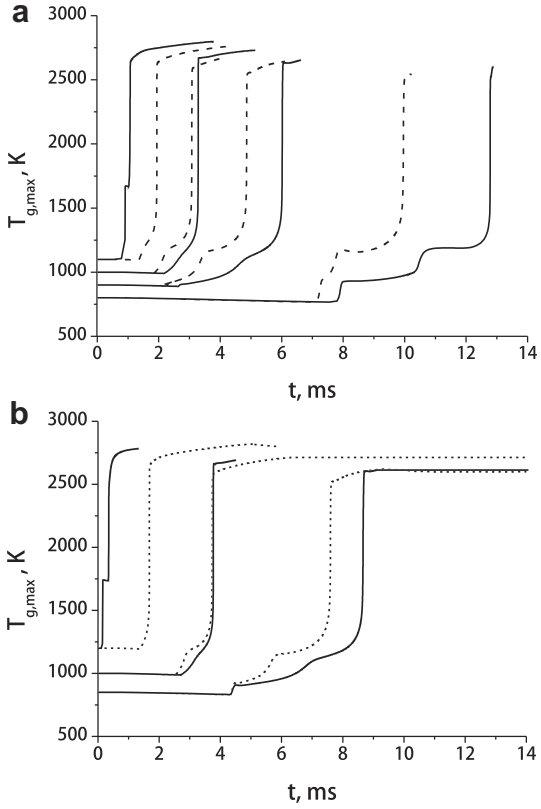

Fig. 8 – Predicted time histories of the maximum gas temperature $T_{g,max}$ in the stoichiometric mixtures *n*-heptane (drops) – hydrogen – air (a) and *n*-decane (drops) – hydrogen – air (b) at different initial temperatures and different initial hydrogen content: 7.5% (vol.) H_2 (solid curves) and 0% H_2 (dashed curves); drop diameter $d_0 = 60$ μm and $P_0 = 20$ atm.

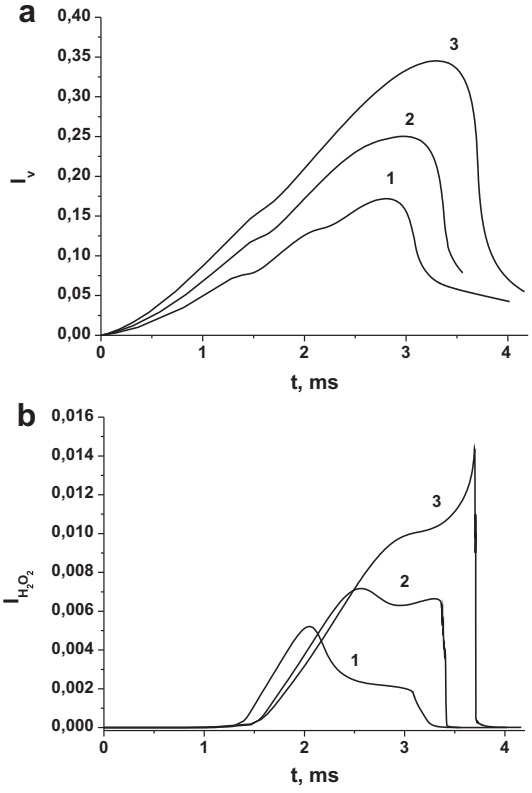

Fig. 9 – Predicted time histories of the normalized mass contents of fuel vapor (a) and hydrogen peroxide (b) around a drop in uniform stoichiometric *n*-heptane drop suspension at different initial volumetric H_2 content: 1 – 0%, 2 – 7.5%, and 3 – 14.5%; $d_0 = 60$ μm and $P_0 = 20$ atm.

example, Fig. 9 shows the time histories of the normalized mass content of fuel vapor I_v (Fig. 9a) and hydrogen peroxide $I_{H_2O_2}$ (Fig. 9b) in the sphere of radius R around the fuel drop in uniform stoichiometric *n*-heptane drop suspension (R is the effective half-distance between drops in gas–drop suspension, see Section 3). The normalized mass content of the ith species in the gas phase is defined as:

$$I_i(t) = m_0^{-1} \int_{r_s(t)}^{R} 4\pi\xi^2 Y_i(\xi, t)\,d\xi \qquad (15)$$

where m_0 is the initial mass of the fuel drop.

The overall self-ignition delay time in Fig. 9 associated with a sharp depletion of fuel vapor and hydrogen peroxide is seen to increase with hydrogen content. Also, addition of increasing amounts of hydrogen to the gas–drop suspension results in faster drop vaporization (caused by high hydrogen specific heat and diffusivity) and larger amounts of fuel vapor and hydrogen peroxide accumulated near the drop before self-ignition occurs. As was mentioned above, such a behavior of the overall self-ignition delay time is caused by reactions of molecular hydrogen with the intermediate products of *n*-heptane oxidation leading to the formation of less active radicals like HO_2.

6. Concluding remarks

The detailed reaction mechanism of *n*-decane oxidation in air was used to simulate self-ignition of stoichiometric homogeneous hydrocarbon–hydrogen–air mixtures and hybrid mixtures of hydrocarbon drops with hydrogen and air at different initial temperature, pressure and volumetric hydrogen content (from 0% to 14.7%). Two hydrocarbons were investigated: *n*-heptane and *n*-decane.

It has been shown that the reactivity of hydrogen-containing mixtures is not always higher than that of the pure hydrocarbon–air mixture. At approximately $T_0 < 1050$ K, addition of hydrogen to hydrocarbon–air mixture was shown to increase the overall self-ignition delay time, i.e. hydrogen plays the role of self-ignition inhibitor. In these conditions, with the increase of hydrogen content in homogeneous and hybrid mixtures the duration of the blue-flame reaction stage was shown to become shorter and even to degenerate. This phenomenon is caused by reactions of molecular hydrogen with the intermediate products of hydrocarbon oxidation leading to the formation of less active species like HO_2 radical hindering chain branching processes. Nevertheless, at approximately $T_0 > 1050$ K, hydrogen addition was shown to decrease the overall self-ignition delay time thus indicating that hydrogen serves as self-ignition promoter. These findings have to be taken into account when discussing the perspectives of

practical applications of fuels blended with hydrogen and relevant explosion safety issues.

Acknowledgments

This work was supported by the Russian Foundation for Basic Research grant 11-08-01297 and Program "Combustion and Explosion" of the Presidium of the Russian Academy of Sciences.

REFERENCES

[1] Verhelst S, Wallner T. Hydrogen-fueled internal combustion engines. Prog Energy Combust Sci 2009;35:490–527.
[2] Karim GA. Combustion in gas fueled compression: ignition engines of the dual fuel type. J Gas Turbine Power 2003;215: 827.
[3] McWilliam L. Combined hydrogen diesel combustion: an experimental investigation into the effects of hydrogen addition on the exhaust gas emissions, particulate matter size distribution and chemical composition. Ph.D. thesis, Brunel University School of Engineering and Design; 2008.
[4] Zhanga Y, Wu J, Ishizuka S. Hydrogen addition effect on laminar burning velocity, flame temperature and flame stability of a planar and a curved CH_4–H_2–air premixed flame. Int J Hydrogen Energy 2009;34:519–27.
[5] Cheng RK, Littlejohn D, Strakey PA, Sidwell T. Laboratory investigations of a low-swirl injector with H_2 and CH_4 at gas turbine conditions. Proc Combust Inst 2009;32(II):3001–9.
[6] Burguburu J, Cabot G, Renou B, Boukhalfa AM, Cazalens M. Effects of H_2 enrichment on flame stability and pollutant emissions for a kerosene/air swirled flame with an aeronautical fuel injector. Proc Combust Inst 2011;33: 2927–35.
[7] Frenillota JP, Cabota G, Cazalens M, Renoua B, Boukhalfa MA. Impact of H_2 addition on flame stability and pollutant emissions for an atmospheric kerosene/air swirled flame of laboratory scaled gas turbine. Int J Hydrogen Energy 2009;34: 3930–44.
[8] Cheng RK, Oppenheim AK. Autoignition in methane–hydrogen mixtures. Combust Flame 1984;58: 125–39.
[9] Basevich VY, Belyaev AA, Medvedev SN, Posvyanskii VS, Frolov SM. Oxidation and combustion mechanisms of paraffin hydrocarbons: transfer from C_1–C_7 to C_8H_{18}, C_9H_{20}, and $C_{10}H_{22}$. Rus J Phys Chem B 2011;5(6):974–90.
[10] Basevich VY, Belyaev AA, Frolov SM. The mechanisms of oxidation and combustion of normal alkane hydrocarbons: the transition from C_1–C_3 to C_4H_{10}. Rus J Phys Chem B 2007; 2(5):477–84.
[11] Basevich VY, Vedeneev VI, Frolov SM, Romanovich LB. Nonextensive principle to construct oxidation and combustion mechanisms of normal alkane hydrocarbons: the transition from C_1–C_2 to C_3H_8. Rus J Chem Phys 2006; 25(11):87.
[12] Basevich VY, Belyaev AA, Frolov SM. Mechanisms of the oxidation and combustion of normal alkanes: the transition from C_1–C_4 to C_5H_{12}. Rus J Phys Chem B 2009;3:629.
[13] Basevich VY, Belyaev AA, Frolov SM. Mechanisms of the oxidation and combustion of normal alkanes: transition from C_1–C_5 to C_6H_{14}. Rus J Phys Chem B 2010;4:634.
[14] Basevich VY, Belyaev AA, Posvyanskii VS, Frolov SM. Mechanism of the oxidation and combustion of normal paraffin hydrocarbons: transition from C_1–C_6 to C_7H_{16}. Rus J Phys Chem B 2010;4:985.
[15] Lidskii BV, Neuhaus MG, VYa Basevich, Frolov SM. On calculation of laminar flame propagation with regard for multicomponent diffusion. Rus J Chem Phys 2003;22(3):51.
[16] Pfahl U, Fieweger K, Adomeit G. Self-ignition of diesel-relevant hydrocarbon–air mixtures under engine conditions. In: Proc. 26th Symp. (Int.) on Comb. Pittsburgh: Combust Inst; 1996. p. 781.
[17] Zhukov VP, Sechenov VA, Starikovskii AY. Autoignition of *n*-decane at high pressure. Combust Flame 2008;153:130.
[18] Troshin KY. Experimental study of the ignition of *n*-hexane- and *n*-decane-based surrogate fuels. Rus J Chem Phys 2008; 2(3):419–25.
[19] Shen HPS, Steinberg J, Vanderover J, Oehlschlaeger MA. A shock tube study of the ignition of *n*-heptane, *n*-decane, *n*-dodecane, and *n*-tetradecane at elevated pressures. Energy Fuels 2009;23(5):2482–9.
[20] Wang H, Warner SJ, Oehlschlaeger A, Bounaceur R, Biet J, Glaude PA, et al. An experimental and kinetic modeling study of the autoignition of α-methylnaphthalene/air and α-methylnaphthalene/*n*-decane/air mixtures at elevated pressures. Combust Flame 2010;157(10):1976–88.
[21] Anagnostou E, Brokaw RS, Butler JN. Effect of concentration on ignition delays for various fuel–oxygen–nitrogen mixtures at elevated temperatures. NACA TN 3887, 1956.
[22] Golovichev VI. Numerical integration of chemical-kinetics equations. Combust Explosion Shock Waves 1973;9(4):418.
[23] Herzler J, Naumann C. Shock-tube study of the ignition of methane/ethane/hydrogen mixtures with hydrogen contents from 0% to 100% at different pressures. Proc Combust Inst 2009;32:213.
[24] Mathieu O, Levacque A, Petersen EL. Effects of N_2O addition on the ignition of H_2–O_2 mixtures: experimental and detailed kinetic modeling study. Int J Hydrogen Energy 2012;37:15393.
[25] Gersen S, Anikin NB, Mokhov AV, Levinsky HB. Int J Hydrogen Energy 2008;33(7):1957.
[26] Mittal G, Sung C-J, Yetter RA. Autoignition of H_2/CO at elevated pressures in a rapid compression machine. Int J Chem Kinet 2006;38:516.
[27] Martynenko VV, Penyaz'kov OG, Ragotner KA, Shabunya SI. High-temperature ignition of hydrogen and air at high pressures downstream of the reflected shock wave. J Eng Phys Thermophysics 2004;77(4):785.
[28] Wang BL, Olivier H, Grönig H. Ignition of shock-heated H_2–air–steam mixtures. Combust Flame 2003;133(1–2):93.
[29] Blumenthal RK, Fieweger K, Komp G, Adomeit H, Gelfand B. Self-ignition of H_2-air mixtures at high pressure and low temperature. In: Proc. 20th Symp. Int. Shock Waves; 1996. p. 935.
[30] Frolov SM, Basevich VY, Frolov FS, Borisov AA, Smetanyuk VA, Avdeev KA, et al. Correlation between drop vaporization and self-ignition. Rus J Chem Phys 2009;28(5): 3–18.
[31] Reid RC, Prausnitz JM, Sherwood TK. The properties of gases and liquids. N.Y.: McGraw–Hill; 1977.
[32] Tanabe M, Bolik T, Eigenbrod C, Rath HJ. Spontaneous ignition of liquid droplets from a view of non-homogeneous mixture formation and transient chemical reactions. Proc Combust Inst 1996;26:1637–43.
[33] Schnaubelt S, Moriue O, Coordes T, Eigenbrod C, Rath HJ. Detailed numerical simulations of the multistage self-ignition process of *n*-heptane, isolated droplets and their verification by comparison with microgravity experiments. Proc Combust Inst 2000;28:953.
[34] Moriue O, Eigenbrod C, Rath HJ, Sato J, Okai K, Tsue M, et al. Effects of dilution by aromatic hydrocarbons on staged ignition behavior of *n*-decane droplets. Proc Combust Inst 2000;28(1):969–75.
[35] Sokolik AS, Basevich VY. On the kinetic nature of self-ignition in diesel engine conditions. Sov J Phys Chem 1954;28: 1935.